

C-terminal Domains of Transmembrane α -Amino-3-hydroxy-5-methyl-4-isoxazole Propionate (AMPA) Receptor Regulatory Proteins Not Only Facilitate Trafficking but Are Major Modulators of AMPA Receptor Function^{*[S]}

Received for publication, July 1, 2009, and in revised form, August 28, 2009. Published, JBC Papers in Press, September 22, 2009, DOI 10.1074/jbc.M109.039891

Charlotte Sager^{‡§}, Jan Terhag^{‡§¶}, Sabine Kott[‡], and Michael Hollmann^{¶1}

From the [‡]Department of Biochemistry I-Receptor Biochemistry, Ruhr University Bochum, the [§]Ruhr University Research School, Ruhr University Bochum, and the [¶]Graduiertenkolleg 736, Deutsche Forschungsgemeinschaft, D-44780 Bochum, Germany

α -Amino-3-hydroxy-5-methyl-4-isoxazole propionate (AMPA)-type glutamate receptors are essential players in fast synaptic transmission in the vertebrate central nervous system. Their synaptic delivery and localization as well as their electrophysiological properties are regulated by transmembrane AMPA receptor regulatory proteins (TARPs). However, the exact mechanisms of how the four originally designated TARPs ($\gamma 2$, $\gamma 3$, $\gamma 4$, and $\gamma 8$) modulate AMPA receptor function remain largely unknown. Previous studies suggested the C-terminal domain (CTD) of $\gamma 2$ to mediate increased trafficking and reduced desensitization of AMPA receptors. As it remained unclear whether these findings extend to other TARPs, we set out to investigate and compare the role of the CTDs of the four original TARPs in AMPA receptor modulation. To address this issue, we replaced the TARP CTDs with the CTD of the homologous subunit $\gamma 1$, a voltage-dependent calcium channel subunit expressed in skeletal muscle that lacks TARP properties. We analyzed the impact of the resulting chimeras on GluR1 functional properties in *Xenopus* oocytes and HEK293 cells. Interestingly, the CTDs of all TARPs not only modulate the extent and kinetics of desensitization but also modulate agonist potencies of AMPA receptors. Furthermore, the CTDs are required for TARP-induced modulation of AMPA receptor gating, including conversion of antagonists to partial agonists and constitutive channel openings. Strikingly, we found a special role of the cytoplasmic tail of $\gamma 4$, suggesting that the underlying mechanisms of modulation of AMPA receptor function are different among the TARPs. We propose that the intracellularly located CTD is the origin of TARP-specific functional modulation and not merely a facilitator of trafficking.

AMPA² receptors mediate the majority of fast excitatory synaptic transmission in the mammalian central nervous sys-

tem. They are ligand-gated ion channels comprising the four members GluR1–GluR4 (1). Four subunits assemble in homo- or heterotetrameric complexes to form functional AMPA receptors (2, 3). Native AMPA receptors have been shown to associate with homologs of the calcium channel subunit $\gamma 1$ such as $\gamma 2$, $\gamma 3$, $\gamma 4$, and $\gamma 8$, which collectively have been termed transmembrane AMPA receptor regulatory proteins (TARPs) (4–6). Very recently, two more homologs of $\gamma 1$, $\gamma 5$ and $\gamma 7$, were additionally identified as a separate family of regulatory proteins named “type II TARPs” (7–8). In the following we focus only on the originally identified TARPs (“type I TARPs”). They regulate synaptic transport and localization and modulate key electrophysiological properties of AMPA receptors (9–11). In particular, TARPs decrease the extent of desensitization and slow desensitization, activation, and deactivation kinetics of AMPA receptors (12–18). Furthermore, they alter pharmacological properties of AMPA receptors such that they increase agonist potencies and efficacies and convert the antagonists 6-cyano-7-nitroquinoxaline-2,3-dione (CNQX) and 6,7-dinitroquinoxaline-2,3-dione (DNQX) into partial agonists of AMPA receptors (12–14, 16, 19–21). Additionally, TARPs increase AMPA receptor mean conductance and decrease the polyamine block, demonstrating their influence on ion channel properties (13, 22).

The detailed mechanisms whereby TARPs modulate AMPA receptor function are not clearly understood. It has been previously suggested that the intracellular C-terminal domain (CTD) of $\gamma 2$ controls AMPA receptor trafficking and desensitization (13–14, 23). Because it has previously been shown that $\gamma 2$ is not the prototypical TARP (16), it remains unclear whether these findings extend to other TARP CTDs. To gain a more detailed insight into the function of the CTDs of TARPs, we replaced the CTD of each of the four original TARPs by that of $\gamma 1$, a calcium channel subunit that is structurally related to TARPs but does not alter AMPA receptor properties. Coexpression analysis of the resulting chimeras with GluR1 showed that the reduction of AMPA receptor desensitization by $\gamma 2$ and

onic kidney; GluR, glutamate receptor; NBQX, 2,3-dihydroxy-6-nitro-7-sulfamoyl-benzo[*f*]quinoxaline-2,3-dione; CNQX, 6-cyano-7-nitroquinoxaline-2,3-dione; DNQX, 6,7-dinitroquinoxaline-2,3-dione; EGFP, enhanced green fluorescent protein; EC₅₀, half-maximal effective concentration; KA, kainate; Glu, glutamate; TCM, trichlormethiazide; NASP, 1-naphthylacetyl spermine; LBD, ligand binding domain.

* This work was supported by Deutsche Forschungsgemeinschaft Grant HO 1118/11-1.

[S] The on-line version of this article (available at <http://www.jbc.org>) contains supplemental Figs. S1 and S2.

¹ To whom correspondence should be addressed: Dept. of Biochemistry I, Receptor Biochemistry, Bldg. NC, Rm. 6/171, Ruhr University Bochum, Universitätsstrasse 150, Bochum D-44780, Germany. Tel.: 49-234-32-24225; Fax: 49-234-32-14244; E-mail: Michael.Hollmann@rub.de.

² The abbreviations used are: AMPA, α -amino-3-hydroxy-5-methyl-4-isoxazole propionate; AMPAR, AMPA receptor; TARP, transmembrane AMPA receptor regulatory protein; CTD, C-terminal domain; HEK, human embry-

TARP C Terminus Is a Functional Modulator

$\gamma 3$ is critically dependent on their CTDs. The modulation of receptor desensitization by $\gamma 4$ and $\gamma 8$, on the other hand, is only slightly influenced by their CTDs. Furthermore, the CTDs of TARPs partly mediate the increase in kainate efficacy and glutamate potency. Interestingly, the C-terminal domains of $\gamma 2$, $\gamma 3$, and $\gamma 8$ are essential to enable activation of AMPA receptors by the antagonists CNQX and DNQX and to induce constitutive channel openings, whereas the CTD of $\gamma 4$ is not essential. Thus, we propose that the specificity with which a TARP modulates an AMPA receptor is determined by its C-terminal domain.

EXPERIMENTAL PROCEDURES

Generation of Constructs—cDNA encoding the rat calcium channel subunit $\gamma 1$ (Cacng1) was cloned from skeletal muscle by reverse transcription-PCR. Total RNA was prepared by the single step method of RNA isolation described by Chomczynski and Sacchi (24). First strand cDNA was synthesized using RevertAidTM H Minus M-MuLV Reverse Transcriptase (Fermentas, St. Leon-Rot, Germany) and the following primers: $\gamma 1$ sense, 5'-GCCGCTCTAGAGCCATGTCACAGACCAAAA-CAGCG-3'; $\gamma 1$ antisense, 5'-CCCGGGGGATCCCTAGTGC-TCTGACTCAGTGTCCA-3'. The primers were designed to fit the published rat $\gamma 1$ sequence (GenBankTM accession number NM_019255) (25). The sense primer contains an XbaI restriction site, the antisense primer contains a BamHI restriction site at the 5'-end to allow directed cloning of the complete cDNA of $\gamma 1$ into pSGEM, an expression vector for *Xenopus* oocytes (26). To ensure full activity of the restriction enzymes, the palindromic sequences were capped by five to six randomly chosen nucleotides. After cloning of the full-length cDNA of $\gamma 1$ into pSGEM, the sequence of the construct was verified by sequencing.

C-terminal chimeras between $\gamma 1$ and the TARPs $\gamma 2$, $\gamma 3$, $\gamma 4$, and $\gamma 8$ were generated via PCR-directed mutagenesis (27). First, chimeric sense primers (42-mer) were designed. The 5' parts of these chimeric primers contain the sequence of the 3'-end of the fourth transmembrane domain of the acceptor sequence. The 3' parts of the primers were identical with the 5' part of the C-terminal domain of the donor sequence. An antisense primer binding in pSGEM was used to amplify a fragment containing the entire sequence of the C-terminal domain of the donor subcloned in pSGEM capped at the 5'-end by 21 nucleotides of the 3'-end of the fourth transmembrane domain of the acceptor. In a second PCR, fragments of the acceptor terminated at the fourth transmembrane domain were generated using appropriate primers. The products from the first two PCRs, which were overlapping and complementary at the fourth transmembrane domains of the acceptor, were combined in overlap extension PCRs. The resulting PCR products were then subcloned into the wild-type acceptors. The C-terminal chimeras were named as follows: acceptor-(exchanged part)donor (e.g. $\gamma 2$ provided with the C-terminal domain of $\gamma 1$ was named $\gamma 2$ -(CT) $\gamma 1$). For subsequent experiments in HEK293 cells, chimeras were C-terminally tagged with enhanced green fluorescent protein (EGFP) by deletion of the stop codon by PCR mutagenesis and cloning of PCR products into

pEGFP-N1 (Clontech, Palo Alto, CA) using KpnI and AgeI restriction sites.

cRNA Synthesis—cRNA synthesis was performed as described previously (28). Briefly, template DNA was linearized with a suitable restriction enzyme. cDNA was transcribed using an *in vitro* transcription kit (Fermentas) with a modified protocol that uses 400 μM ^{m7}GpppG (New England Biolabs, Frankfurt am Main, Germany) for capping and an extended reaction time of 3 h with T7 polymerase. Transcripts were trace-labeled with α -[³²P]UTP to allow calculation of yields and evaluation of transcript quality by formaldehyde agarose gel electrophoresis.

Electrophysiological Measurements in *Xenopus laevis* Oocytes—Oocytes were surgically removed from the ovaries of *X. laevis* (Nasco, Fort Atkinson, WI) anesthetized with 3-aminobenzoic acid ethylester (1.5 g/liter, Sigma-Aldrich). The follicular cell layer was removed with 784 units/ml (4 mg/ml) collagenase type I (Worthington, Lakewood, NJ) in Ca²⁺-free Barth's solution (88 mM NaCl, 1.1 mM KCl, 2.4 mM NaHCO₃, 0.8 mM MgSO₄, 15 mM HEPES-NaOH, pH 7.6) with slow agitation for 1.5 h at 20 °C. After incubation, the oocytes were washed extensively with Barth's solution (88 mM NaCl, 1.1 mM KCl, 2.4 mM NaHCO₃, 0.3 mM Ca(NO₃)₂, 0.4 mM CaCl₂, 0.8 mM MgSO₄, 15 mM HEPES-NaOH, pH 7.6). Oocytes of stages V and VI were selected and maintained in Barth's solution containing 100 $\mu\text{g}/\text{ml}$ gentamicin, 40 $\mu\text{g}/\text{ml}$ streptomycin, and 63 $\mu\text{g}/\text{ml}$ penicillin. Defolliculated oocytes were injected with 4 ng of receptor cRNA and 0.4 ng TARP cRNA using a nanoliter injector (World Precision Instruments, Sarasota, FL). 4–5 days after injection, agonist-induced current responses from oocytes were recorded in magnesium frog Ringer's solution (115 mM NaCl, 2.5 mM KCl, 1.8 mM MgCl₂, 10 mM HEPES-NaOH, pH 7.2) under voltage clamp at -70 -mV holding potential with a TurboTec 10CX amplifier (npi electronic, Tamm, Germany) controlled by Pulse software (HEKA, Lambrecht, Germany). Recording electrodes were pulled from borosilicate glass (Hilgenberg, Malsfeld, Germany) using a PIP5 pipette vertical puller (HEKA). Electrodes were filled with 3 M KCl and had resistances of 0.5–1.5 M Ω (voltage electrode) or 0.1–1.5 M Ω (current electrode). Agonists were applied for 20 s by superfusion at a flow rate of 5 ml/min. To determine EC₅₀ values for glutamate, nine different agonist concentrations were applied to the same oocyte. The data from each oocyte were fitted separately, and EC₅₀ values from four to five oocytes were averaged. The presented data are reported as mean \pm S.E., and the statistical significance was determined with an unpaired Student's *t* test.

Isolation of Cell Surface Proteins—Glycosylated cell surface proteins were labeled with biotinylated concanavalin A and selectively isolated from *Xenopus* oocytes by affinity purification using streptavidin-agarose. Intact oocytes were incubated in 10 μM biotinyl-concanavalin A (Sigma-Aldrich) in normal frog Ringer's solution (115 mM NaCl, 2.5 mM KCl, 1.8 mM CaCl₂, 10 mM HEPES-NaOH, pH 7.2) for 30 min at room temperature. After washing five times for 10 min in normal frog Ringer's solution, intact oocytes were homogenized in ice-cold H buffer (20 $\mu\text{l}/\text{oocyte}$, 100 mM NaCl, 20 mM Tris-HCl, pH 7.4, 1% Triton X-100, plus a mixture of protease inhibitors (CompleteTM tablets, Roche Applied Science)) and incubated for 1 h

at 4 °C on a rotator. After centrifugation for 15 min at 16,000 × *g* and 4 °C, the supernatants were supplemented with 20 μl of streptavidin-agarose beads (Fluka, Buchs, Switzerland) and incubated at 4 °C for 3 h on the rotator. The streptavidin-agarose beads were then pelleted by centrifugation for 5 min at 16,000 × *g* and 4 °C, washed three times in H buffer, and finally boiled in 20 μl of SDS-PAGE loading buffer (6 M urea, 0.8 M β-mercaptoethanol, 6% SDS, 20% glycerol, 25 mM Tris-HCl, pH 6.8, 0.1% bromophenol blue).

Gel Electrophoresis and Western Blotting—Proteins were separated on SDS-polyacrylamide gels using the Mini-Protean®3 system (Bio-Rad, Munich, Germany). On each gel, the amounts of protein were equal in all lanes. This was achieved by using the identical numbers of oocytes for each sample. The separated proteins were then transferred to Hybond ECL nitrocellulose membranes (Amersham Biosciences). The membranes were blocked for 3 h with 1× Roti-Block solution (Roth, Karlsruhe, Germany) in TBS-T (140 mM NaCl, 20 mM Tris-HCl, pH 7.6, 0.1% Tween 20) and then incubated overnight at 4 °C with rabbit anti-GluR1, which was a kind gift of Richard L. Huganir (Dept. of Neuroscience, Howard Hughes Medical Institute, The Johns Hopkins University School of Medicine, Baltimore, MD). After washing with TBS-T containing 0.1× Roti-Block solution, the membrane was incubated for 1 h at 4 °C with a horseradish peroxidase-conjugated goat anti-rabbit antibody (Sigma-Aldrich). Immunoreactive bands were visualized by enhanced chemiluminescence (Super Signal West Pico, Pierce). Visualized bands were quantified using the software ImageJ (National Institutes of Health).

Electrophysiological Measurements in HEK293 Cells—Human embryonic kidney 293 (HEK293) cells were cultured in the Joklik modification of minimum essential medium Eagle containing 10% fetal bovine serum (Invitrogen), at 37 °C and 8% CO₂ in polyornithine-coated 35-mm dishes. Before transfection, medium was changed to Dulbecco's modified Eagle's medium (Invitrogen), containing 10% fetal bovine serum. Cells were transfected with 2.5 μg of cDNA with an equimolar ratio of AMPA receptor cDNA cloned into pcDNA3.0 and either an enhanced cyan fluorescent protein-tagged TARP or an EGFP-tagged chimeric TARP or pEGFP. Transfections were performed for 6 h at 37 °C and 8% CO₂ using Metafectene (Biontex, Martinsried, Germany). After incubation, the cells were washed with phosphate-buffered saline before changing back to Joklik modification of minimum essential medium Eagle. 48–72 h after transfection, whole cell patch clamp recordings were performed using an EPC-9 amplifier (HEKA) controlled by Pulse 8.70 software (HEKA). Currents were digitized with a sampling rate of 10 kHz and filtered at 3 kHz. Recording electrodes were pulled from borosilicate glass (GC150TL-10, Harvard Apparatus, Edenbridge, UK) using a PIP5 pipette vertical puller (HEKA). Electrodes were filled with 130 mM CsF, 4 mM NaCl, 1 mM MgCl₂, 0.5 mM CaCl₂, 11 mM EGTA, and 10 mM HEPES, adjusted to pH 7.3 with KOH, and had resistances of 4–8 MΩ. Drugs were prepared in extracellular solution (140 mM NaCl, 4 mM KCl, 2 mM CaCl₂, 1 mM MgCl₂, 10 mM HEPES-NaOH, pH 7.3) and were applied using a theta glass capillary (Hilgenberg) mounted on a piezoelectric controller (Physik Instrumente, Karlsruhe, Germany). Time constants were calcu-

lated by single exponential fits using Pulse Fit 8.7 (HEKA). The extent of desensitization was calculated as the ratio of steady-state to peak glutamate-evoked currents.

RESULTS

The C-terminal Domain of TARPs Critically Influences the Modulation of Electrophysiological Properties and Trafficking of GluR1(Q)flip—Stargazin (γ2) has been shown to modulate AMPA receptor trafficking and desensitization via its CTD (13, 14, 23). To study whether this applies to all TARPs and whether the CTDs are responsible for TARP-specific differences in modulation of AMPA receptor function, we replaced the CTDs of TARPs by that of γ1, a protein that is homologous to TARPs (20.9% sequence identity between γ2 and γ1 at the protein level) but does not alter the electrophysiological properties of GluR1(Q)flip, and coexpressed the resulting chimeras (TARP-(CT)γ1) with GluR1(Q)flip in *Xenopus* oocytes for functional analysis (Fig. 1). Consistent with literature data, wild-type TARPs increased glutamate- and kainate-induced current responses of GluR1(Q)flip to different extents (Fig. 1, A and B, and Table 1) by increasing receptor trafficking and kainate efficacy, and decreasing the extent of receptor desensitization (12–14, 15–17). Each of the TARP/γ1 chimeras also increased glutamate- and kainate-induced currents of GluR1(Q)flip but to a significantly smaller extent than the respective wild-type TARP (Fig. 1, A and B, and Table 1). Moreover, the potentiation of kainate-induced currents was nearly identical for all TARP-(CT)γ1 chimeras (Fig. 1A and Table 1), demonstrating a loss of TARP-specific modulation. On the other hand, glutamate-induced currents were differentially potentiated by the TARP-(CT)γ1 chimeras, indicating that some TARP-specific properties are preserved: γ2-(CT)γ1 and γ3-(CT)γ1 increased glutamate-induced currents equally and very weakly (1.8 ± 0.3-fold and 2.3 ± 0.4-fold, respectively), whereas γ8-(CT)γ1 and γ4-(CT)γ1 had considerably larger and divergent effects (10.9 ± 2.2-fold and 42.4 ± 6.3-fold, respectively). Because it has been reported that the CTD of γ2 is an important determinant of AMPA receptor trafficking (13, 23), we investigated whether the observed differential modulatory effects of TARP-(CT)γ1 chimeras compared with wild-type TARPs can be attributed to differences in surface expression levels of GluR1(Q)flip.

First, we investigated whether TARPs and our C-terminal chimeras influence the total protein expression levels of GluR1(Q)flip receptors in *Xenopus* oocytes. Western blot analysis revealed that coexpression of wild-type TARP and TARP-(CT)γ1 chimeras produced either no or only very small changes (maximally by a factor of 1.6 in the case of γ4 and γ4-(CT)γ1) in total protein expression of GluR1(Q)flip (Fig. 1C). This means that any significant wild-type TARP- or chimeric TARP-mediated increase in surface-incorporated GluR1(Q)flip receptor number must be caused by an up-regulation of trafficking efficiency rather than by a simple up-regulation in the bulk amount of protein available for trafficking.

However, 5 days after injection of cRNA there was hardly any difference in surface-incorporated GluR1(Q)flip receptors in the absence or in the presence of wild-type TARPs or TARP-(CT)γ1 chimeras (Fig. 1, C and D). Thus, at least after 5 days of continued expression it appears that no significant TARP-me-

TARP C Terminus Is a Functional Modulator

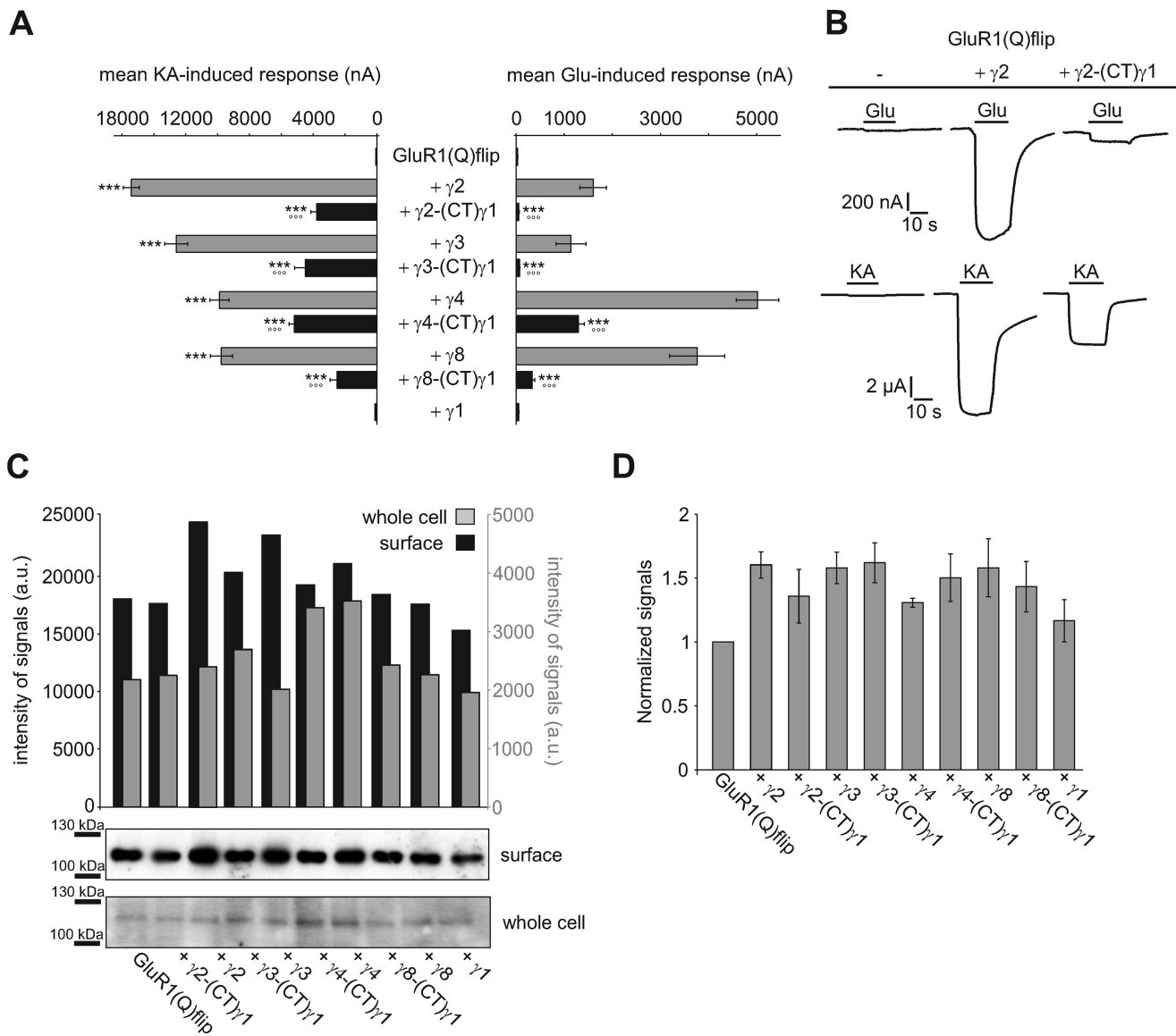


FIGURE 1. Substitution of the C-terminal domain affects TARP function. *A*, mean current responses of GluR1(Q)flip in coexpression with wild-type and chimeric TARPs carrying the C-terminal domain of $\gamma 1$, recorded in *Xenopus* oocytes 5 days after injection. Concentrations of the applied agonists were 300 μ M glutamate (Glu) and 150 μ M kainate (KA). Each bar represents the mean (\pm S.E.) of 13–18 oocytes. Black asterisks show significant differences compared with GluR1(Q)flip; open circles show differences of TARP chimeras compared with respective wild-type TARPs (***) and (oo), $p < 0.005$; Student's *t* test). *B*, representative current responses of GluR1(Q)flip alone and in coexpression with $\gamma 1$ and its C-terminal chimera with $\gamma 1$. The duration of agonist application is indicated by horizontal black bars. *C* and *D*, Western blot analysis of whole cell and surface-incorporated GluR1(Q)flip alone and together with wild type as well as chimeric TARPs 5 days after cRNA injection into *X. laevis* oocytes. The data shown represent three independent experiments. *C*, representative Western blot out of three performed. On each gel, the amount of protein loaded corresponds to identical numbers of oocytes for all samples. Shown are Western blot analyses of purified surface protein fractions (10 oocytes each) and whole cell total protein preparations (1/2 oocyte each, limited by the large total protein content). *D*, quantification of surface protein determined from Western blot. The values were normalized to GluR1(Q)flip in the absence of wild-type or chimeric TARPs. Each bar represents the mean (\pm S.E.) of three different experiments.

diated additional increase in AMPA receptor surface expression occurs in *Xenopus* oocytes. Because this finding appears to contradict the TARP-mediated increase in surface expression of AMPA receptors reported in the literature based on measurements 2 or 3 days after cRNA injection (23, 29–31), we considered that the increase of AMPA receptor expression induced by TARPs may be time-dependent. Therefore, we determined the effects of $\gamma 2$ and the $\gamma 2$ -(CT) $\gamma 1$ chimera on the time course of GluR1(Q)flip surface expression from 1 day to 5 days after cRNA injection of *Xenopus* oocytes (Fig. 2). Western blot analysis revealed that between 1 and 4 days after cRNA injection $\gamma 2$, but not the $\gamma 2$ -(CT) $\gamma 1$ chimera, robustly increased the amount

of surface-incorporated GluR1(Q)flip receptors (Fig. 2). We confirmed this observation also for $\gamma 3$ and its C-terminal chimera at day 3 after injection (supplemental Fig. S1). By contrast, no TARP-induced increase in surface-incorporated GluR1(Q)flip was observed on day 5 (Figs. 1C and 2). Evidently, the TARP-mediated increase in AMPA receptor surface expression in *Xenopus* oocytes is a kinetic effect, with TARPs speeding up the expression at the plasma membrane without increasing the maximal level of expressed receptor. It appears that the plasma membranes of cRNA-injected *Xenopus* oocytes become saturated with GluR1 channels, masking any potential differences in surface expression. To support this observation,

we additionally performed electrophysiological recordings of GluR1(Q)flip at different time points after injection. Indeed, no significant changes in kainate-induced currents were observed from 4 to 6 days of expression (supplemental Fig. S2).

Given the observation that $\gamma 2$ led to a 4.7-fold increase in surface-incorporated GluR1(Q)flip receptors 4 days after injection and only 1.6-fold increase 5 days after injection (Figs. 1C and 2), it is very obvious that alterations in GluR1(Q)flip surface expression cannot explain the large potentiation of glutamate- and kainate-induced currents (52.5 ± 10.9 -fold and 211.9 ± 24.2 -fold, respectively (Table 1)). Because we detected no alteration of surface-incorporated GluR1(Q)flip in coexpression with the $\gamma 2$ -(CT) $\gamma 1$ chimera on day 4 or day 5 of expression,

TABLE 1

Effects on glutamate- and kainate-induced GluR1(Q)flip currents of wild-type and chimeric TARPs carrying the C-terminal domain of $\gamma 1$

Potentiation factors of glutamate- and kainate-induced currents (\pm S.E.) of GluR1(Q)flip in absence and presence of wild-type and chimeric TARPs. The ratios of kainate- to glutamate-induced currents (I_{KA}/I_{Glu}) were calculated for each oocyte and averaged (\pm S.E.).

	Potentiation factors		I_{KA}/I_{Glu} ratio (<i>n</i>)
	I_{Glu} (<i>n</i>)	I_{KA} (<i>n</i>)	
GluR1(Q)flip	1.0 ± 0.0 (17)	1.0 ± 0.0 (17) ^a	2.9 ± 0.5 (17)
+ $\gamma 1$	1.3 ± 0.3 (13)	1.3 ± 0.3 (13)	2.4 ± 0.3 (13)
+ $\gamma 2$	52.5 ± 10.9 (14) ^a	211.9 ± 24.2 (14) ^a	13.2 ± 1.9 (14) ^a
+ $\gamma 2$ -(CT) $\gamma 1$	1.8 ± 0.3 (15) ^{a,b}	51.9 ± 7.6 (15) ^{a,b}	75.0 ± 7.1 (15) ^{a,b}
+ $\gamma 3$	37.3 ± 11.2 (15) ^a	173.2 ± 21.4 (15) ^a	20.4 ± 2.9 (15) ^a
+ $\gamma 3$ -(CT) $\gamma 1$	2.3 ± 0.4 (15) ^{a,b}	61.7 ± 11.6 (15) ^{a,b}	67.0 ± 11.4 (15) ^{a,b}
+ $\gamma 4$	164.4 ± 24.1 (18) ^a	135.8 ± 17.1 (18) ^a	2.1 ± 0.2 (18)
+ $\gamma 4$ -(CT) $\gamma 1$	42.4 ± 6.3 (18) ^{a,b}	71.3 ± 9.0 (18) ^{a,b}	4.3 ± 0.2 (18) ^{b,c}
+ $\gamma 8$	123.4 ± 23.6 (13) ^a	134.2 ± 17.5 (13) ^a	3.0 ± 0.3 (13)
+ $\gamma 8$ -(CT) $\gamma 1$	10.9 ± 2.2 (14) ^{a,b}	34.3 ± 7.1 (14) ^{a,b}	7.7 ± 0.7 (14) ^{a,b}

^a Significant difference compared with GluR1(Q)flip; $p < 0.005$; Student's *t*-test.

^b Significant difference of TARP chimeras compared with respective wild-type TARPs; $p < 0.005$; Student's *t*-test.

^c Significant difference compared with GluR1(Q)flip; $p < 0.05$; Student's *t*-test.

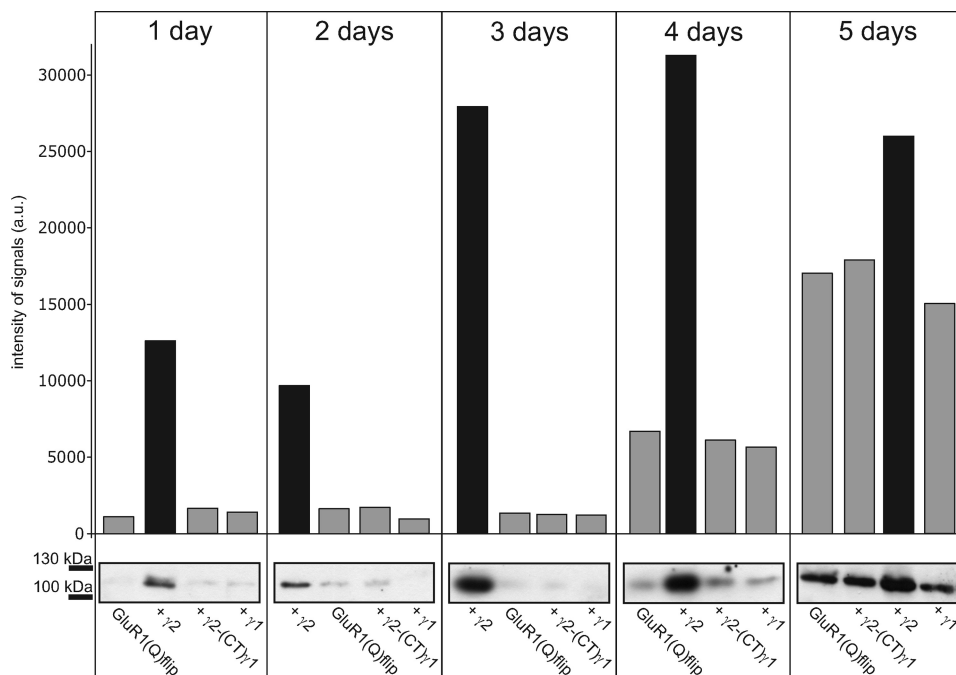


FIGURE 2. Impact of $\gamma 2$ and its C-terminal chimera on the time course of GluR1(Q)flip surface expression. Western blot analysis of surface-incorporated GluR1(Q)flip receptors in absence and presence of $\gamma 2$ and the $\gamma 2$ / $\gamma 1$ chimera 1–5 days after injection of cRNA in *Xenopus* oocytes. This experiment was performed on a batch of oocytes different from the batches used for Fig. 1, C and D. In each lane, the amount of protein corresponds to identical numbers of oocytes ($n = 20$ oocytes). The bar diagram shows quantification of Western blot results.

even the weaker potentiation of glutamate- and kainate-induced currents by the $\gamma 2$ / $\gamma 1$ chimera (1.8 ± 0.3 -fold and 51.9 ± 7.6 -fold, respectively (Fig. 1A and Table 1)) must be attributed to mechanisms other than protein trafficking.

The independence of the electrophysiological modulation of AMPA receptors by TARPs from TARP effects on trafficking has previously been noted (13, 16). Therefore, we next calculated the ratio of kainate- to glutamate-induced responses (I_{KA}/I_{Glu} ratio). Changes in this ratio indicate altered electrophysiological properties of GluR1 and are independent of changes in surface expression. The TARPs $\gamma 2$ and $\gamma 3$ increase this ratio, but the extent differs depending on the associated TARP. The TARPs $\gamma 4$ and $\gamma 8$ produce no increase (Table 1). The TARP-(CT) $\gamma 1$ chimeras increased the I_{KA}/I_{Glu} ratio of GluR1 even stronger than the respective wild-type TARPs (Table 1). Interestingly, this additional increase was larger with the $\gamma 2$ -(CT) $\gamma 1$ and $\gamma 3$ -(CT) $\gamma 1$ chimeras than with the $\gamma 4$ -(CT) $\gamma 1$ and $\gamma 8$ -(CT) $\gamma 1$ chimeras (Table 1). From this data it appears likely that the TARP CTDs play an essential role in mediating the modulation of electrophysiological properties of GluR1.

The C-terminal Domains of TARPs Determine TARP-specific Modulation of AMPA Receptor Desensitization—Next, we investigated which factors cause the additional increase in I_{KA}/I_{Glu} ratios of GluR1 in coexpression with the TARP-(CT) $\gamma 1$ chimeras. Increased I_{KA}/I_{Glu} ratios can be caused by either an elevated relative kainate efficacy (*i.e.* I_{KA} increases) or less potentiated glutamate-induced currents due to a persistent, strong desensitization (*i.e.* I_{Glu} decreases).

A hallmark of TARPs is their ability to decrease the extent of AMPA receptor desensitization (12–15, 16–17). For $\gamma 2$, this effect is dependent on its CTD, as shown in truncation experiments (14). To investigate whether the CTDs of the other TARPs play a similar role in the inhibition of desensitization, we analyzed the impact of our TARP-(CT) $\gamma 1$ chimeras on the desensitization of GluR1(Q)flip by applying the desensitization inhibitor trichlormethiazide (TCM, $600 \mu M$) together with the agonist glutamate. A strong potentiation of glutamate-induced currents by TCM points to a strongly desensitizing receptor, whereas a weaker potentiation indicates a weakly desensitizing receptor. For GluR1(Q)flip, TCM potentiated glutamate-induced current responses 100 ± 8.6 -fold (Fig. 3, A and B). Wild-type TARPs considerably reduced the potentiation by TCM, $\gamma 4$ and $\gamma 8$ even stronger (to 2.9 ± 0.3 -fold and 4.2 ± 0.5 -fold, respectively) than $\gamma 2$ and $\gamma 3$ (to 14.9 ± 2.4 -fold and 24.7 ± 3.6 -fold, respectively) (Fig. 3, A and B). These data support the proposed subdivision of TARPs into two subfamilies

TARP C Terminus Is a Functional Modulator

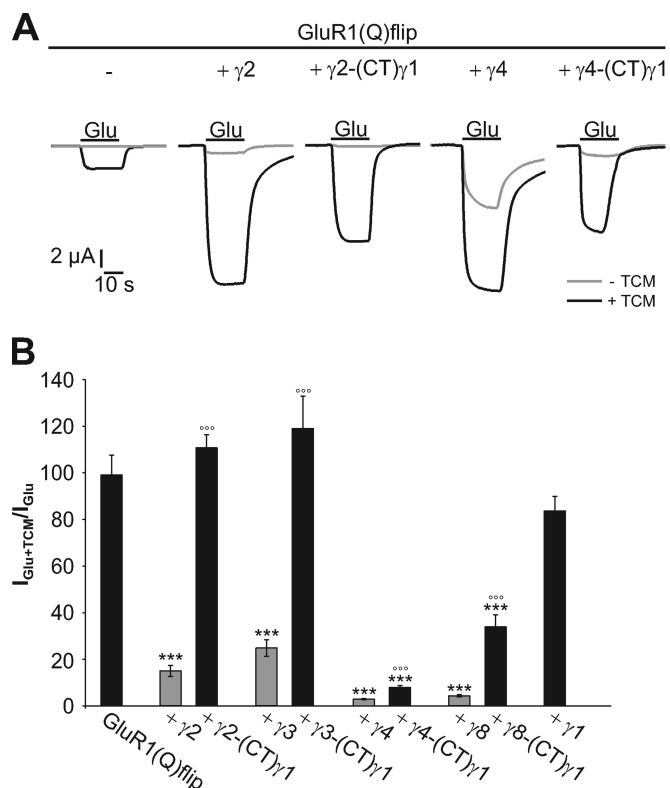


FIGURE 3. Influence of TARP C-terminal chimeras with γ 1 on the extent of desensitization of GluR1(Q)flip. *A*, typical current responses elicited by application of 300 μ M glutamate in the absence and presence of 600 μ M TCM of GluR1(Q)flip alone and in coexpression with γ 2, γ 4, and their respective C-terminal chimeras with γ 1 recorded in *Xenopus* oocytes. *Black bars* indicate duration of agonist application. *B*, $I_{\text{Glu+TCM}}/I_{\text{Glu}}$ ratios for GluR1(Q)flip alone and in coexpression with wild-type and chimeric TARPs carrying the CTD of γ 1 were calculated for each oocyte and averaged (\pm S.E.; *** p < 0.005 significantly different from GluR1(Q)flip alone; °°°, p < 0.005 significantly different compared with wild-type TARPs; Student's *t* test; n = 13–18 oocytes).

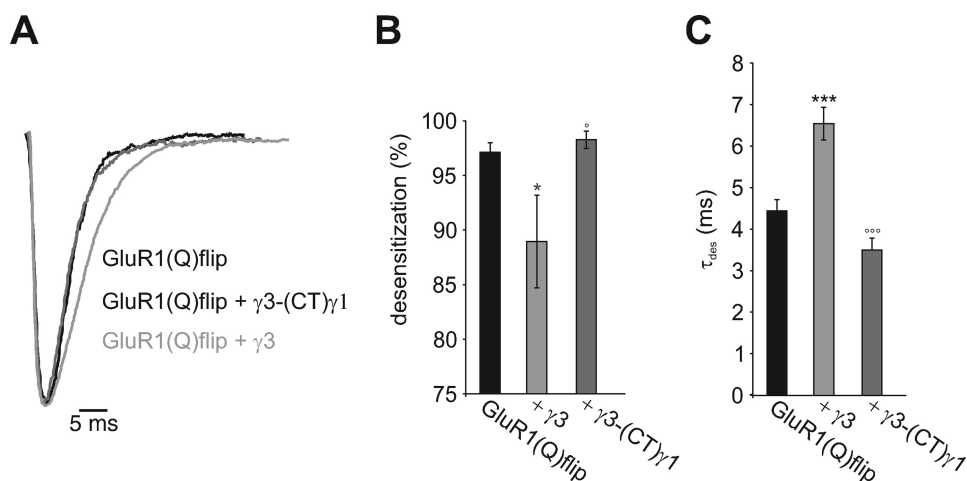


FIGURE 4. Patch clamp analysis of desensitization kinetics of GluR1(Q)flip coexpressed with γ 3 and chimeric γ 3 carrying the CTD of γ 1. *A*, glutamate-induced (3 mM) whole cell responses of GluR1(Q)flip in the absence and presence of γ 3 and the γ 3/ γ 1 chimera. The current responses are normalized and aligned to the peak current. *B*, extent of desensitization of GluR1(Q)flip during coexpression of either γ 3 or the γ 3/ γ 1 chimera. *C*, desensitization time constants of GluR1(Q)flip during coexpression of γ 3 and the γ 3/ γ 1 chimera. *Bars* represent means \pm S.E. (n = 5–14; *, p < 0.05; *** p < 0.005 significantly different from GluR1(Q)flip alone; °, p < 0.05; °°°, p < 0.005 significantly different compared with wild-type γ 3; Student's *t*-test; n = 5–14).

(15, 18). Interestingly, this subdivision persists in the TARP-(CT) γ 1 chimeras, but on a different level: γ 2-(CT) γ 1 and γ 3-(CT) γ 1 did not affect the potentiation of glutamate-induced responses by TCM at all, while γ 4-(CT) γ 1 and γ 8-(CT) γ 1 still reduced it, albeit to a lesser extent than the respective wild-type TARPs (to 9.3 ± 0.8 -fold and 33.7 ± 5.1 -fold, respectively (Fig. 3*B*)). Hence, γ 4-(CT) γ 1 and γ 8-(CT) γ 1 still reduced receptor desensitization to some extent, whereas γ 2-(CT) γ 1 and γ 3-(CT) γ 1 didn't.

TARPs not only reduce the extent of receptor desensitization but also slow down its kinetics (12–15, 17–18). To investigate whether the CTD influences this property as well, we coexpressed GluR1(Q)flip with either γ 3 or the chimera γ 3-(CT) γ 1 in HEK293 cells and performed whole cell patch clamp measurements using a fast perfusion system to detect fast kinetics. We confirmed fast and nearly complete desensitization of glutamate-induced currents for GluR1(Q)flip. This desensitization was reduced and slowed by wild-type TARPs as expected (Fig. 4 and Table 2). By contrast, γ 3-(CT) γ 1 did not alter desensitization at all, confirming the results from *Xenopus* oocytes (Fig. 4 and Table 2). To summarize, the reduction of AMPAR desensitization by γ 2 and γ 3 is critically dependent on their CTDs, whereas the CTDs of γ 4 and γ 8 only partly contribute to the reduction of desensitization. Although we showed that γ 1 did not alter the electrophysiological properties of AMPA receptors, it cannot be ruled out that this was merely a consequence of lack of interaction with the receptor (Fig. 1). Thus, one might speculate that the CTD of γ 1 could potentially modulate AMPA receptor function when it becomes associated with the receptor via our TARP-(CT) γ 1 chimeras. However, we can exclude this possibility as we showed that the chimeras γ 2-(CT) γ 1 and γ 3-(CT) γ 1 failed to alter the desensitization of GluR1. Therefore, we can conclude that our results are due to the absence of the CTD of TARPs rather than the presence of the CTD of γ 1. Furthermore, to exclude the possibility that

our results are merely an artifact of constructing chimeric TARPs with γ 1, we replaced the CTD of γ 2 by that of γ 4. This experiment was designed to investigate the properties of TARP CTDs in the modulation of AMPA receptor desensitization in more detail. We coexpressed the γ 2-(CT) γ 4 chimera, the wild-type TARPs γ 2 and γ 4, and the γ 2-(CT) γ 1 chimera with GluR1(Q)flip for functional analysis in *Xenopus* oocytes. Interestingly, the chimera γ 2-(CT) γ 4 increased glutamate-induced currents to a significantly smaller extent than wild-type γ 2 or γ 4 but produced a considerably larger effect than the γ 2-(CT) γ 1 chimera (Fig. 5, *A* and *B*). To test whether this differential potentiation of glutamate-induced currents was due to altered desensi-

TABLE 2**Effects of $\gamma 3$ and the $\gamma 3$ -(CT) $\gamma 1$ chimera on glutamate-evoked currents and desensitization kinetics of GluR1(Q)flip**

Mean (\pm S.E.) peak and steady-state glutamate-evoked current responses, extent of desensitization, and desensitization time constants of GluR1(Q)flip alone and in coexpression with either $\gamma 3$ or its C-terminal chimera with $\gamma 1$ are shown. The extent of desensitization (%) is given by $100\% - (I_{\text{steady state}}/I_{\text{peak}}) \times 100\%$.

	I_{Glu} (peak) (n)	I_{Glu} (steady state) (n)	Desensitization	τ_{des} (n)
	<i>pA</i>	<i>pA</i>	%	<i>ms</i>
GluR1(Q)flip	804.1 \pm 221.7 (14)	39.7 \pm 26.0 (14)	97.1 \pm 0.9 (14)	4.45 \pm 0.27 (14)
+ $\gamma 3$	3357.8 \pm 447.2 (5) ^a	433.8 \pm 208.3 (5) ^a	88.9 \pm 4.3 (5) ^b	6.54 \pm 0.39 (5) ^a
+ $\gamma 3$ -(CT) $\gamma 1$	1783.3 \pm 414.3 (7) ^{a,c}	24.3 \pm 8.4 (7) ^d	98.3 \pm 0.8 (7) ^d	3.50 \pm 0.29 (5) ^c

^a $p < 0.005$, significantly different from GluR1(Q)flip alone.

^b $p < 0.05$, significantly different from GluR1(Q)flip alone.

^c $p < 0.005$, significantly different compared with wild-type $\gamma 3$.

^d $p < 0.05$, significantly different compared with wild-type $\gamma 3$.

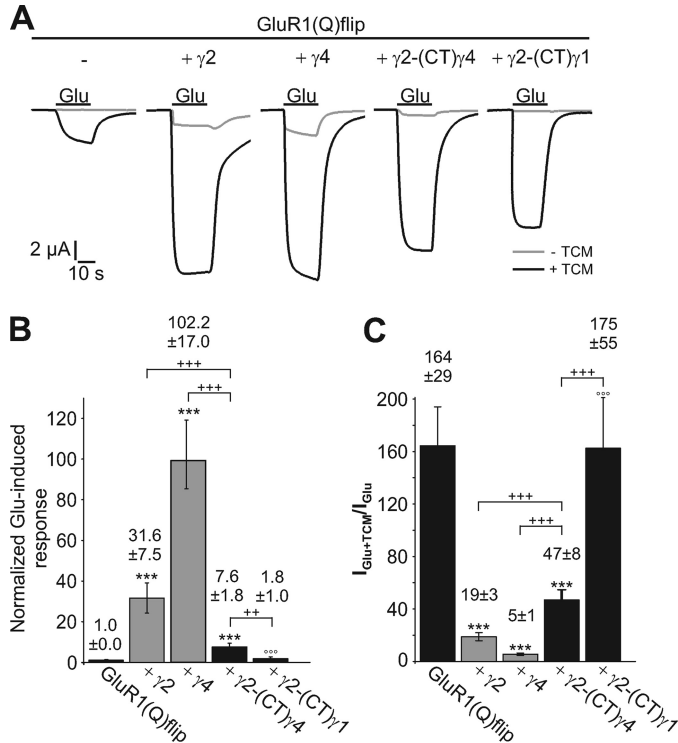


FIGURE 5. Influence of $\gamma 2$ carrying the C-terminal domain of $\gamma 4$ on the extent of desensitization of GluR1(Q)flip. *A*, typical current responses of GluR1(Q)flip elicited by the application of 300 μM glutamate (Glu) in *Xenopus* oocytes in the absence (gray traces) and presence (black traces) of 600 μM TCM; analyzed were the receptor alone and in coexpression with $\gamma 2$, $\gamma 4$, and the two chimeras $\gamma 2$ -(CT) $\gamma 1$ and $\gamma 2$ -(CT) $\gamma 4$. Duration of Glu application is indicated by black bars. *B*, normalized glutamate-induced responses of GluR1(Q)flip in coexpression with $\gamma 2$, $\gamma 4$, and the two chimeras $\gamma 2$ -(CT) $\gamma 1$ and $\gamma 2$ -(CT) $\gamma 4$ (\pm S.E.). *C*, $I_{\text{Glu+TCM}}/I_{\text{Glu}}$ ratios for GluR1(Q)flip alone and in coexpression with $\gamma 2$, $\gamma 4$, $\gamma 2$ -(CT) $\gamma 1$, and $\gamma 2$ -(CT) $\gamma 4$ were calculated for each oocyte and averaged (\pm S.E.). Black asterisks show significant differences compared with GluR1(Q)flip; open circles show differences of TARP chimeras compared with respective wild-type TARPs; plus symbols show differences of $\gamma 2$ -(CT) $\gamma 4$ to $\gamma 2$ and $\gamma 4$ (+, $p < 0.01$; +++, $p < 0.005$; +, $p < 0.05$; Student's *t* test; $n = 5-14$).

tization properties of GluR1(Q)flip, we applied the desensitization inhibitor TCM as described before. Contrary to $\gamma 2$ -(CT) $\gamma 1$, which did not alter the potentiation of glutamate-induced currents by TCM, the chimera $\gamma 2$ -(CT) $\gamma 4$ still reduced it, albeit to a smaller extent than wild-type $\gamma 2$ or $\gamma 4$ (Fig. 5C). Thus, while $\gamma 2$ -(CT) $\gamma 4$ was still capable of reducing AMPA receptor desensitization, $\gamma 2$ -(CT) $\gamma 1$ was not. We can conclude from these data that the CTD of $\gamma 4$ provides some reduction of desensitization, an effect that can be transferred to a chimera with the N-terminal part of $\gamma 2$ that by itself doesn't alter receptor desensitization at all. This proves that the CTD of $\gamma 4$

TABLE 3**Effects of wild-type and chimeric TARPs carrying the C-terminal domain of $\gamma 1$ on relative kainate efficacy and glutamate potency of GluR1(Q)flip**

Relative kainate efficacies ($I_{\text{KA}}/I_{\text{Glu+TCM}}$) (150 μM KA, 300 μM Glu, and 600 μM TCM) and glutamate potencies of GluR1(Q)flip in the absence and presence of the four original TARPs and the TARP/ $\gamma 1$ chimeras were calculated for each oocyte and averaged (\pm S.E.).

	$I_{\text{KA}}/I_{\text{Glu+TCM}}$ ratio (n)	EC_{50} Glu (n)
		μM
GluR1(Q)flip	0.03 \pm 0.01 (16)	24.2 \pm 1.7 (7)
+ $\gamma 1$	0.04 \pm 0.01 (13)	20.4 \pm 5.3 (3)
+ $\gamma 2$	0.91 \pm 0.02 (14) ^a	3.8 \pm 0.5 (9) ^a
+ $\gamma 2$ -(CT) $\gamma 1$	0.67 \pm 0.05 (15) ^{a,b}	10.0 \pm 1.4 (5) ^{a,b}
+ $\gamma 3$	0.92 \pm 0.04 (15) ^a	1.7 \pm 0.2 (3) ^a
+ $\gamma 3$ -(CT) $\gamma 1$	0.53 \pm 0.07 (15) ^{a,b}	15.3 \pm 2.5 (4) ^{c,d}
+ $\gamma 4$	0.78 \pm 0.02 (14) ^a	7.5 \pm 0.6 (3) ^a
+ $\gamma 4$ -(CT) $\gamma 1$	0.49 \pm 0.02 (17) ^{a,b}	12.6 \pm 1.3 (5) ^{a,e}
+ $\gamma 8$	0.74 \pm 0.02 (13) ^a	8.2 \pm 0.1 (3) ^a
+ $\gamma 8$ -(CT) $\gamma 1$	0.27 \pm 0.03 (14) ^{a,b}	13.9 \pm 0.2 (3) ^{b,c}

^a $p < 0.005$, significantly different compared with GluR1(Q)flip alone.

^b $p < 0.005$, significantly different from wild-type TARPs.

^c $p < 0.05$, significantly different compared with GluR1(Q)flip alone.

^d $p < 0.01$, significantly different from wild-type TARPs.

^e $p < 0.05$, significantly different from wild-type TARPs.

directly contributes to the reduction of desensitization of the coexpressed GluR1(Q)flip, confirming our results obtained with the TARP-(CT) $\gamma 1$ chimeras.

The TARP-mediated Increase in Kainate Efficacy Is Influenced but Not Determined by Their C-terminal Domains—The second factor that influences $I_{\text{KA}}/I_{\text{Glu}}$ ratio is the efficacy of the partial agonist kainate. TARPs have been shown to increase this efficacy (13–14, 16–17), resulting in a stronger potentiation of kainate-induced compared with glutamate-induced currents, and consequently in increased $I_{\text{KA}}/I_{\text{Glu}}$ ratios. To investigate whether the CTDs of TARPs play a role in this modulation of kainate efficacy, we analyzed the impact of the TARP-(CT) $\gamma 1$ chimeras on kainate efficacies at GluR1(Q)flip.

To this end, we calculated the kainate-induced currents relative to glutamate-induced currents in the presence of TCM ($I_{\text{KA}}/I_{\text{Glu+TCM}}$) to eliminate the influence of differential modulation of desensitization. For GluR1(Q)flip we observed small $I_{\text{KA}}/I_{\text{Glu+TCM}}$ ratios of 0.03 ± 0.01 (Table 3), reflecting ~ 36 -fold smaller currents induced by kainate compared with glutamate, in the presence of TCM. As expected, wild-type TARPs increased $I_{\text{KA}}/I_{\text{Glu+TCM}}$ ratios, indicating increased relative kainate efficacies (Table 3). The two TARPs $\gamma 2$ and $\gamma 3$ caused more pronounced increases in relative kainate efficacies than $\gamma 4$ and $\gamma 8$ (Table 3), again confirming the two functionally distinct subfamilies of TARPs. All in all TARP-(CT) $\gamma 1$ chimeras still increased relative kainate efficacies, yet to a lesser extent than the wild-type TARPs (Table 3). This finding indicates that

TARP C Terminus Is a Functional Modulator

the CTDs of TARPs are not essential for the modulation of kainate efficacy, but influence its extent. Moreover, the additional increase in I_{KA}/I_{Glu} ratio observed with the TARP-(CT) $\gamma 1$ chimeras compared with wild-type TARPs (Table 1) is solely attributable to the weaker reduction of desensitization, as kainate efficacy is even decreased.

The TARP-specific Increase in Glutamate Potency Can Be Attributed to Their C-terminal Domains—Previous studies have revealed that TARPs increase agonist potencies (12–13, 16, 19, 20). However, the underlying mechanisms have not been previously investigated. To this end, we examined whether the CTDs of TARPs play a role in increasing agonist potencies.

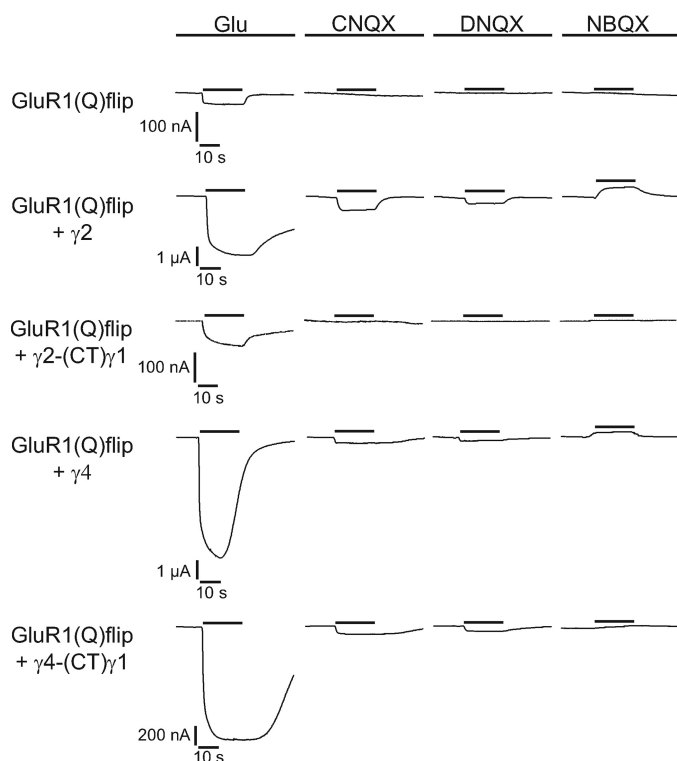


FIGURE 6. The CTDs of TARPs control conversion of AMPA receptor antagonists to partial agonists. Representative glutamate ($300 \mu\text{M}$), CNQX ($10 \mu\text{M}$), DNQX ($10 \mu\text{M}$), and NBQX ($10 \mu\text{M}$)-induced current responses of GluR1(Q)flip in the absence and presence of each of the four original TARPs and the TARP-(CT) $\gamma 1$ chimeras. Black bars indicate duration of application of glutamate and antagonists. Note different scaling.

TABLE 4

Modulatory effects on AMPA receptor antagonist action of wild-type and chimeric TARPs carrying the C-terminal domain of $\gamma 1$

Mean (\pm S.E.) glutamate ($300 \mu\text{M}$), CNQX ($10 \mu\text{M}$), DNQX ($10 \mu\text{M}$), and NBQX ($10 \mu\text{M}$)-induced current responses of GluR1(Q)flip in the absence and presence of each of the four original TARPs and the TARP-(CT) $\gamma 1$ chimeras are shown.

	I_{Glu} (n)	I_{CNQX} (n)	I_{DNQX} (n)	I_{NBQX} (n)	$I_{CNQX+TCM}$ (n)
			nA		
GluR1(Q)flip	52 \pm 8 (12)	0 \pm 0 (14)	1 \pm 0 (11)	1 \pm 1 (12)	8.8 \pm 2.1 (7)
+ $\gamma 1$	43 \pm 8 (10)	0 \pm 0 (14)	1 \pm 0 (10)	0 \pm 0 (10)	6.3 \pm 1.4 (7)
+ $\gamma 2$	2603 \pm 390 (13) ^a	239 \pm 55 (14) ^a	134 \pm 40 (12) ^a	-382 \pm 111 (13) ^a	3506 \pm 292 (10) ^a
+ $\gamma 2$ -(CT) $\gamma 1$	85 \pm 19 (15) ^b	1 \pm 1 (18) ^b	2 \pm 1 (12) ^b	-7 \pm 3 (15) ^{b,c}	30.8 \pm 12.2 (8) ^b
+ $\gamma 3$	1282 \pm 122 (14) ^a	48 \pm 7 (14) ^a	24 \pm 7 (13) ^a	-76 \pm 13 (14) ^a	1280 \pm 122 (9) ^a
+ $\gamma 3$ -(CT) $\gamma 1$	93 \pm 17 (14) ^b	1 \pm 1 (17) ^b	1 \pm 0 (14) ^b	-1 \pm 1 (14) ^b	13.0 \pm 4.2 (14) ^b
+ $\gamma 4$	4267 \pm 350 (10) ^a	122 \pm 25 (10) ^a	58 \pm 16 (9) ^a	-281 \pm 98 (10) ^a	3258 \pm 408 (10) ^a
+ $\gamma 4$ -(CT) $\gamma 1$	2571 \pm 319 (10) ^b	25.4 \pm 8.9 (18) ^{a,b}	32 \pm 11 (8) ^c	-83 \pm 23 (10) ^c	1401 \pm 299 (13) ^{a,b}
+ $\gamma 8$	3795 \pm 701 (10) ^a	46 \pm 13 (10) ^a	22 \pm 5 (9) ^a	-105 \pm 38 (9) ^a	2241 \pm 539 (9) ^a
+ $\gamma 8$ -(CT) $\gamma 1$	113 \pm 13 (15) ^b	1 \pm 1 (18) ^b	1 \pm 1 (14) ^b	-4 \pm 1 (15) ^{b,d}	23.5 \pm 5.6 (13) ^b

^a $p < 0.005$, significantly different compared with GluR1(Q)flip alone.

^b $p < 0.005$, significantly different from wild-type TARPs.

^c $p < 0.01$, significantly different compared with GluR1(Q)flip alone.

^d $p < 0.05$, significantly different compared with GluR1(Q)flip alone.

Therefore, we determined EC_{50} values for glutamate of GluR1(Q)flip coexpressed with either TARP-(CT) $\gamma 1$ chimeras or wild-type TARPs (Table 3). As we have previously shown (16), $\gamma 2$ and $\gamma 3$ strongly reduced the EC_{50} value for glutamate, whereas $\gamma 4$ and $\gamma 8$ had a less pronounced effect (Table 3). Remarkably, all TARP-(CT) $\gamma 1$ chimeras reduced the EC_{50} value for glutamate as well, but to a lesser extent than the respective wild-type TARPs and all to nearly the same level (Table 3). This suggests that the CTDs determine the TARP-specific portion of the modulation of glutamate potencies, whereas other domains provide a constant portion of modulation common to all TARPs.

Activation of AMPA Receptors by Antagonists Is Controlled via the C-terminal Domains of TARPs—As competitive antagonists for AMPA receptors, quinoxalinediones have been widely used to study excitatory synaptic transmission (32). Although CNQX and DNQX induce a small closure of the AMPA receptor ligand binding cleft (21, 33), these conformational changes are insufficient to open the ion channel. However, in the presence of a TARP both antagonists induce small AMPA receptor-mediated responses in *Xenopus* oocytes as well as in neurons (20–21). Thus, it appears that TARPs alter gating of AMPA receptors such that they can be activated by CNQX and DNQX. Unraveling the underlying mechanisms would be an important step toward understanding how TARPs modulate AMPA receptor function. To address this issue, we tested whether the CTDs of TARPs determine the conversion of CNQX and DNQX from antagonists to agonists of AMPA receptors. In the presence of TARPs, we detected small GluR1(Q)flip-mediated responses upon CNQX and DNQX application (Fig. 6 and Table 4), which were potentiated by TCM (Table 4). By contrast, GluR1(Q)flip could not be activated by either CNQX or DNQX when it was coexpressed with the C-terminal TARP chimeras of $\gamma 2$, $\gamma 3$, and $\gamma 8$ (Fig. 6 and Table 4). For $\gamma 4$ -(CT) $\gamma 1$ we found a different behavior: this chimera, unlike the other three chimeras, is still able to convert CNQX and DNQX to GluR1 agonists (Fig. 6 and Table 4). However, CNQX- and DNQX-induced currents were smaller when GluR1 was coexpressed with $\gamma 4$ -(CT) $\gamma 1$ than upon coexpression with wild-type $\gamma 4$ (79 and 45% reductions, respectively, compared with $\gamma 4$ coexpression).

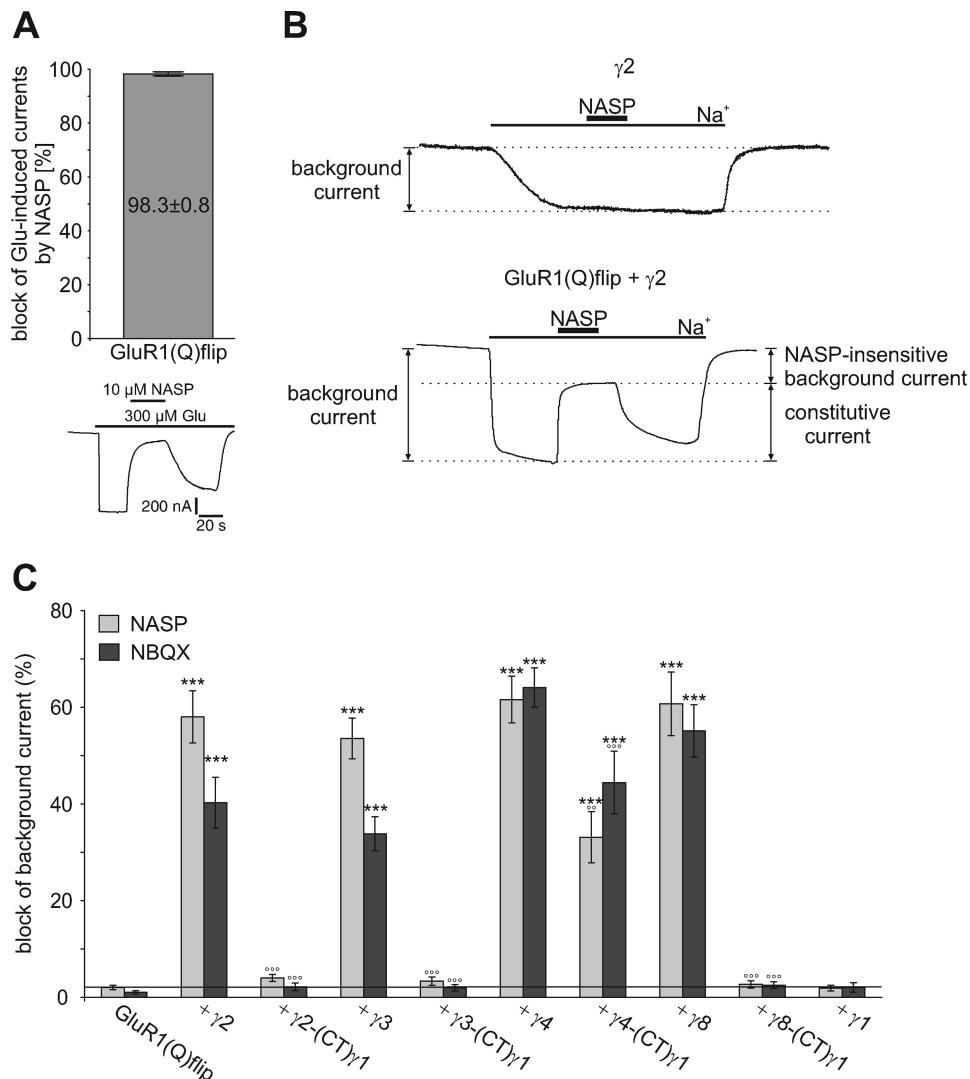


FIGURE 7. Influence of wild-type and chimeric TARPs carrying the C-terminal domain of $\gamma 1$ on constitutive channel openings of GluR1(Q)flip. *A*, mean block of glutamate-induced responses by 10 μM NASP of GluR1(Q)flip ($n = 7$). Data are shown as means (\pm S.E.). Additionally, a representative block of glutamate-induced responses by 10 μM NASP of GluR1(Q)flip is presented. The duration of agonist and NASP application is indicated by horizontal black bars. *B*, typical holding current trace of $\gamma 2$ alone and GluR1(Q)flip coexpressed with $\gamma 2$ in sodium-free Ringer's solution. Application of sodium-containing Ringer's solution triggered an inward current that could be partially blocked by NASP (10 μM , duration of application noted by black bar), thus indicating the fraction of constitutively open GluR1(Q)flip channels. *C*, mean block of background currents by NASP (gray columns) and NBQX (black columns), each at 10 μM , of GluR1(Q)flip alone and coexpressed with wild-type TARPs and TARP/ $\gamma 1$ C-terminal chimeras. The horizontal line marks the level of NASP block of GluR1(Q)flip alone. Data are shown as mean (\pm S.E.) of 10–14 oocytes (***, $p < 0.005$, significantly different from GluR1(Q)flip alone; °°, $p < 0.01$ and °°, $p < 0.005$, significantly different compared with wild-type TARPs; Student's *t*-test).

We conclude from these data that the CTDs of $\gamma 2$, $\gamma 3$, and $\gamma 8$ are decisive for the conversion of CNQX and DNQX to partial agonists. Remarkably, the CTD of $\gamma 4$ is only partly responsible for this conversion.

Substitution of the C-terminal Domain Disrupts TARP-mediated Constitutive Openings of GluR1 Channels—Although CNQX and DNQX induce inward currents at GluR1 in the presence of TARPs, the AMPAR competitive antagonist NBQX induces apparent outward currents, suggesting the presence of constitutively open GluR1 channels that are inhibited by NBQX (Table 4) (20, 21). The NBQX-induced apparent outward currents were smaller upon coexpression of TARP-(CT) $\gamma 1$ chimeras, suggesting that the CTD is involved in this effect. To investigate this further, we first recorded background currents (= holding currents at -70 mV in the absence of agonist) of oocytes expressing GluR1(Q)flip alone or together with either wild-type TARPs or the TARP-(CT) $\gamma 1$ chimeras. Coexpression of wild-type TARPs significantly raised background currents of GluR1(Q)flip-expressing oocytes (data not shown). To determine whether this increase in background current is caused by constitutively open GluR1 channels, we applied the AMPAR open-channel blocker NASP, which completely blocks GluR1(Q)flip channels at a concentration of 10 μM (Fig. 7, *A* and *B*). Thus, a block of background currents by NASP reflects open GluR1 channels in the absence of agonist. This approach is well established to distinguish between true constitutively open GluR1 channels and additional components potentially caused by recording procedures (34).

We observed that NASP blocks ~60% of TARP-induced background currents ($58.0 \pm 5.4\%$ for $\gamma 2$, $53.5 \pm 4.2\%$ for $\gamma 3$, $61.6 \pm 4.8\%$ for $\gamma 4$, and $60.7 \pm 6.6\%$ for $\gamma 8$), demonstrating that these currents are indeed at least partially attributable to constitutively open GluR1 channels (Fig. 7, *B* and *C*).

We next used NBQX to investigate whether the constitutive currents may be caused by conformational changes in the ligand binding domain of AMPA receptors (34). We found that TARP-induced background currents can be blocked by NBQX in a TARP-specific manner (Fig. 7*B*). Interestingly, $\gamma 2$ - and $\gamma 3$ -induced background currents were inhibited by NBQX to a lesser extent ($40.7 \pm 5.4\%$ and $33.9 \pm 3.5\%$, respectively) than $\gamma 4$ - and $\gamma 8$ -induced background currents ($64.1 \pm 4.1\%$ and $55.1 \pm 5.4\%$, respectively). Remarkably, the fraction of constitutively open GluR1 channels in the presence of $\gamma 4$ and $\gamma 8$ appears to be completely blocked by NBQX, as suggested by the observation that NASP and NBQX blocked background currents to the same extent (Fig. 7*B*). In the presence of $\gamma 2$ or $\gamma 3$, on the other hand, NBQX blocked a considerably smaller part of the background current than NASP. These findings again confirm the proposed division of the four TARPs into two functionally distinct groups and suggest different mechanisms of interaction/modulation with AMPA receptors for these two

TARP C Terminus Is a Functional Modulator

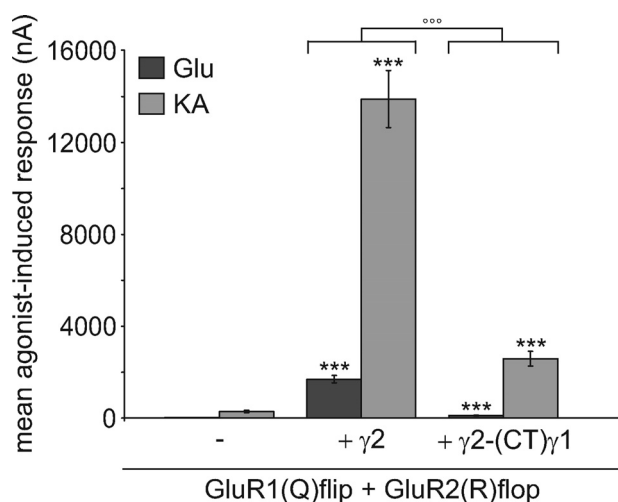


FIGURE 8. Influence of $\gamma 2$ and chimeric $\gamma 2$ carrying the CTD of $\gamma 1$ on agonist-induced currents of heteromeric GluR1(Q)flip/GluR2(R)flop receptors. Mean glutamate- and kainate-induced responses of GluR1(Q)flip/GluR2(R)flop receptors in coexpression with $\gamma 2$ and its C-terminal chimera recorded 4 days after injection of cRNA in *Xenopus* oocytes. Concentrations of the applied agonists were 300 μM glutamate (Glu) and 150 μM kainate (KA). Each bar represents the mean (\pm S.E.) of 9 or 10 oocytes. Black asterisks show significant differences compared with GluR1(Q)flip/GluR2(R)flop; open circles show differences of chimeric $\gamma 2$ compared with wildtype $\gamma 2$ (***) and (***) ($p < 0.005$; Student's *t* test). The assembly of heteromeric receptor complexes was verified by analysis of current-voltage relationships taking advantage of the linear current-voltage relationship of receptor complexes containing edited (R) receptor variants.

groups. It appears that all four original TARPs lead to a more efficient translation of conformational changes in the LBD to channel opening, so that random movement of the LBD is sufficient for channel opening. Additionally, only $\gamma 2$ and $\gamma 3$ appear to induce constitutive channel openings of GluR1(Q)flip uncoupled from the LBD conformational state. Remarkably, these TARP-induced alterations of GluR1 gating are in most cases abolished when the CTD is replaced by that of $\gamma 1$, suggesting that the CTDs of TARPs are essential for these effects. However, the $\gamma 4$ -(CT) $\gamma 1$ chimera still induced background currents that were blocked by NASP and NBQX to the same extent ($33.1 \pm 5.3\%$ block by NASP and $44.4 \pm 6.5\%$ block by NBQX), although these currents were smaller than in the presence of wild-type $\gamma 4$ (Fig. 7B). This observation supports the notion that the CTD of $\gamma 4$ contributes only partly to the modulation of AMPA receptor gating.

Modulation of Heteromeric AMPA Receptors by $\gamma 2$ Depends on Its C-terminal Domain—So far we investigated the impact of our TARP-(CT) $\gamma 1$ chimeras only on homomeric GluR1(Q)flip receptors. Because AMPA receptors naturally occur as heteromeric assemblies mainly built from combinations of GluR1 or GluR3 with an edited GluR2 variant in both splice isoforms (35–37), we examined whether the C-terminal domain of $\gamma 2$ is also responsible for the modulation of the physiologically important heteromeric GluR1(Q)flip/GluR2(R)flop receptors. For *Xenopus* oocytes expressing this heteromeric receptor subunit combination we detected robust current amplitudes 4 days after injection (21.1 ± 2.5 nA for glutamate and 286.4 ± 57.9 nA for kainate) (Fig. 8). Consistent with the literature data, wild-type $\gamma 2$ increased glutamate- and kainate-induced current responses of this heteromeric AMPA receptor (Fig. 8) (16). We

observed a clear increase of ~ 80 -fold for glutamate-induced responses to 1696 ± 163 nA and an increase of ~ 50 -fold for kainate-induced responses to 14725 ± 1070 nA. The $\gamma 2$ -(CT) $\gamma 1$ chimera increased glutamate- and kainate-induced currents of the heteromeric AMPA receptor combination GluR1(Q)flip/GluR2(R)flop as well but to a significantly smaller extent than wild-type $\gamma 2$ (~ 5 -fold increase to 110 ± 14 nA and ~ 10 -fold increase to 2587 ± 322 nA, respectively) (Fig. 8). The $\gamma 2$ -(CT) $\gamma 1$ chimera showed the same tendency in modulating agonist-induced currents of homomeric GluR1(Q)flip receptors, suggesting that our findings concerning modulation of homomeric AMPA receptors are relevant to physiological conditions.

DISCUSSION

The CTDs of TARPs play an important role in the modulation of AMPAR trafficking and function by TARPs. However, to disclose the function of this particular domain previous studies have focused only on $\gamma 2$ as the prototypical TARP, neglecting possible differences between the members of the TARP family. Therefore, we studied the role of the CTDs of the four original TARPs $\gamma 2$, $\gamma 3$, $\gamma 4$, and $\gamma 8$ by substituting them with the CTD of $\gamma 1$ and analyzing the resulting TARP-(CT) $\gamma 1$ chimeras in coexpression with AMPARs in *Xenopus* oocytes and HEK293 cells.

The CTDs of $\gamma 2$ and $\gamma 3$ Are Essential for Increasing AMPAR Trafficking—Several studies have shown that the CTD of $\gamma 2$ contains PDZ-binding sites for synaptic scaffolding proteins and additional endoplasmic reticulum export signals necessary and sufficient for AMPAR trafficking (23, 29–31). Thus, exchanging the CTD of stargazin should result in less increased amounts of AMPARs in the plasma membrane compared with wild-type stargazin. We demonstrated that the effects of TARPs on AMPA receptor surface expression are kinetic effects depending on the duration of expression of the injected cRNA in *Xenopus* oocytes. Therefore, the wild-type TARP-mediated increase and the tiny $\gamma 2$ -(CT) $\gamma 1$ - and $\gamma 2$ -(CT) $\gamma 1$ -mediated increase in plasma membrane-incorporated GluR1 receptors is only observable at the early stages of expression. Such a time dependence of TARP-mediated increase in AMPA receptor trafficking has been described before (38), and we suggest that this phenomenon is due to a saturation of the oocyte membrane after long duration of expression. This effect thus masks any potential alteration in trafficking of AMPA receptors when time points late after the start of expression are investigated.

The CTDs of TARPs Differentially Influence TARP-mediated Inhibition of AMPAR Desensitization—It is well known that TARPs decrease the extent and slow the kinetics of AMPAR desensitization (12–15, 17–18). In truncation experiments, the CTD of $\gamma 2$ has been shown to be essential for the inhibition of AMPAR desensitization (14). We confirm this result for $\gamma 2$ with our chimeric approach and demonstrate that the CTD of $\gamma 3$ has the same importance for the inhibition of AMPAR desensitization. By contrast, the CTDs of $\gamma 4$ and $\gamma 8$ are only partly responsible for the modulation of desensitization, because our $\gamma 4$ -(CT) $\gamma 1$ and $\gamma 8$ -(CT) $\gamma 1$ chimeras were still able to decrease desensitization to some extent, and $\gamma 2$ -(CT) $\gamma 4$ did not produce the same extent of reduction of desensitization as wild-type $\gamma 4$. These findings support the previously proposed subdivi-

sion of TARPs into two subfamilies and suggest that this subdivision is based on molecular/structural differences in the CTD.

The mechanism by which TARPs decrease AMPAR desensitization is still unknown. The two conceivable causes of reduced desensitization are the stabilization of the receptor's open state and the destabilization of its desensitized state (12, 14). We favor the second explanation because destabilization of the desensitized state has been suggested to occur in GluR1 and GluR2 mutants carrying an arginine to glutamate point mutation outside the LBD in the short linker B sequence (39). These mutants display slightly slowed desensitization kinetics, but a strong decrease in the extent of desensitization, presumably caused by electrostatic interactions of the linker and the LBD, thus destabilizing the desensitized state. Interestingly, the arginine to glutamate mutation slows desensitization by only 2-fold, a value very similar to the effect of $\gamma 2$ and $\gamma 3$ on GluR1; $\gamma 4$ and $\gamma 8$ have slightly larger effects (15, 17–18). By contrast, stabilization of the LBD dimer interface by the Leu to Tyr mutation slows desensitization much more strongly, by ~ 30 -fold (40, 41). From these data it appears attractive to speculate that TARPs may destabilize the desensitized state, perhaps by an interaction with the linkers connecting the transmembrane domains with the LBD.

The CTDs of TARPs Contribute to TARP-mediated Changes in Agonist Potencies and Efficacies—TARPs alter electrophysiological as well as pharmacological properties of AMPARs. They differentially increase agonist potencies and more strikingly the efficacy of partial agonists (12–14, 16, 19, 20). Here, we demonstrate that the CTDs of all four TARPs contribute to these effects.

All four TARP-(CT) $\gamma 1$ chimeras still increased the relative kainate efficacy at GluR1(Q)flip, yet less strongly than the respective wild-type TARPs. Likewise, all TARP-(CT) $\gamma 1$ chimeras increased glutamate potency to a lesser extent and to the same level, a distinct difference to the wild-type TARPs. This finding indicates that the CTD is responsible for the TARP-specific portion of modulation of glutamate potency. Yet other domains have to account for the less specific portion of modulation that persists even when the CTD is exchanged. The most obvious candidate for this function is the first extracellular loop, which has previously been implicated in the increase of kainate efficacy (14).

The CTDs of TARPs Are Critical for TARP-mediated Conversion of Certain AMPAR Antagonists to Agonists as Well as for Constitutive Channel Opening—Another effect of TARPs on AMPAR pharmacology is the conversion of the antagonists CNQX and DNQX to partial agonists (20–21, 42). Here we demonstrate that the CTDs of $\gamma 2$, $\gamma 3$, and $\gamma 8$ are essential for this conversion, whereas $\gamma 4$ still has some residual conversion capability when its CTD is exchanged for that of $\gamma 1$. Because a recent study showed that the first extracellular loop of $\gamma 2$ is essential for the conversion as well (42), it can be concluded that these two domains act synergistically in changing the structure of AMPARs such that antagonists can activate them.

A third antagonist, NBQX, does not activate AMPARs in the presence of TARPs but induces small apparent outward currents (20–21, 32). This observation has been suggested to be attributable to TARP-induced constitutive channel openings

that are inhibited by NBQX (20). Here, we show that TARPs induce constitutive channel opening of GluR1 via two mechanisms. The first mechanism appears to be the modification of gating such that random movements of the LBD are sufficient to open the channel. Although this mechanism is common to all TARPs, $\gamma 2$ and $\gamma 3$ cause additional channel openings independent of the LBD conformational state. Conceivably, these two TARPs induce additional constitutively open GluR1 channels via direct interaction with the ion pore or by directly separating the linker regions. For $\gamma 2$, $\gamma 3$, and $\gamma 8$, the CTDs are essential to modify AMPAR gating, whereas $\gamma 4$ retains part of its modulatory function when its CTD is replaced with that of $\gamma 1$. Thus, the mechanism by which $\gamma 4$ alters AMPAR gating does not rely on one single domain and is therefore more robust than that of the other TARPs. This special property might reflect the special physiological role of $\gamma 4$, which is the predominant TARP during early development of the central nervous system, a period critical for the formation of synapses (6).

Possible Sites of AMPAR-TARP Interaction—Agonist efficacy at AMPARs correlates with the degree of agonist-induced closure of the ligand binding cleft, agonist potency correlates with the stability of cleft closure, and desensitization correlates with the stability of the LBD dimer interface (29, 41, 43, 44). Therefore, the TARP-mediated increase in agonist efficacy and affinity as well as the reduction of desensitization could all be explained by direct interactions between the TARP and the AMPAR LBD, increasing and stabilizing cleft closure and stabilizing the dimer interface (20, 45). Nevertheless, interactions of TARPs with the transmembrane domains of AMPARs or the linkers connecting the transmembrane domains with the LBD have also been suggested (5). Interactions of TARPs with the linkers now seem quite likely, because several mutations in the linker B of AMPARs mimic effects of TARPs, e.g. the slowing of desensitization (arginine to glutamate mutation), the conversion of antagonists to partial agonists (lurcher mutation), and the constitutive channel opening (lurcher mutation) (34, 46–47). However, this is difficult to reconcile with the significant role we observed for the CTD, which is located on the other side of the membrane. Interactions between the CTDs on the intracellular side of the membrane might be important for establishing an overall structure of the AMPAR/TARP complex that enables proper interactions between the extracellular domains and thus proper modulation of pharmacological properties. It also appears very likely, that the CTDs of TARPs interact directly with the pore region of AMPARs, because we detected for $\gamma 2$ and $\gamma 3$ an NBQX-insensitive but NASP-sensitive portion of GluR1 background currents. It is also possible that a direct interaction of the TARP CTDs with the CTDs of AMPA receptors can cause modulation of pharmacological properties via allosteric mechanisms.

Acknowledgments—We thank Prof. Dr. Lutz Pott (Dept. of Physiology, Ruhr University Bochum) for providing rat muscle tissue and HEK293 cells. We also thank Christina Klein for preparing HEK293 cell cultures, Björn Peters for expert oocyte preparations, and Daniel Tapken for critical reading and helpful discussions in preparing the manuscript.

REFERENCES

- Hollmann, M., and Heinemann, S. (1994) *Annu. Rev. Neurosci.* **17**, 31–108
- Rosenmund, C., Stern-Bach, Y., and Stevens, C. F. (1998) *Science* **280**, 1596–1599
- Hollmann, M. (1999) *Ionotropic Glutamate Receptors in the CNS*, Springer, Berlin, pp. 3–98
- Vandenberghe, W., Nicoll, R. A., and Brecht, D. S. (2005) *Proc. Natl. Acad. Sci. U.S.A.* **102**, 485–490
- Nakagawa, T., Cheng, Y., Ramm, E., Sheng, M., and Walz, T. (2005) *Nature* **433**, 545–549
- Tomita, S., Chen, L., Kawasaki, Y., Petralia, R. S., Wenthold, R. J., Nicoll, R. A., and Brecht, D. S. (2003) *J. Cell Biol.* **161**, 805–816
- Kato, A. S., Zhou, W., Milstein, A. D., Knierman, M. D., Siuda, E. R., Dotzlaw, J. E., Yu, H., Hale, J. E., Nisenbaum, E. S., Nicoll, R. A., and Brecht, D. S. (2007) *J. Neurosci.* **27**, 4969–4977
- Kato, A. S., Siuda, E. R., Nisenbaum, E. S., and Brecht, D. S. (2008) *Neuron* **59**, 986–996
- Nicoll, R. A., Tomita, S., and Brecht, D. S. (2006) *Science* **311**, 1253–1256
- Ziff, E. B. (2007) *Neuron* **53**, 627–633
- Sager, C., Tapken, D., Kott, S., and Hollmann, M. (2009) *Neuroscience* **158**, 45–54
- Priel, A., Kolleker, A., Ayalon, G., Gillor, M., Osten, P., and Stern-Bach, Y. (2005) *J. Neurosci.* **25**, 2682–2686
- Tomita, S., Adesnik, H., Sekiguchi, M., Zhang, W., Wada, K., Howe, J. R., Nicoll, R. A., and Brecht, D. S. (2005) *Nature* **435**, 1052–1058
- Turetsky, D., Garringer, E., and Patneau, D. K. (2005) *J. Neurosci.* **25**, 7438–7448
- Cho, C. H., St-Gelais, F., Zhang, W., Tomita, S., and Howe, J. R. (2007) *Neuron* **55**, 890–904
- Kott, S., Werner, M., Körber, C., and Hollmann, M. (2007) *J. Neurosci.* **27**, 3780–3789
- Körber, C., Werner, M., Kott, S., Ma, Z. L., and Hollmann, M. (2007) *J. Neurosci.* **27**, 8442–8447
- Milstein, A. D., Zhou, W., Karimzadegan, S., Brecht, D. S., and Nicoll, R. A. (2007) *Neuron* **55**, 905–918
- Yamazaki, M., Ohno-Shosaku, T., Fukaya, M., Kano, M., Watanabe, M., and Sakimura, K. (2004) *Neurosci. Res.* **50**, 369–374
- Kott, S., Sager, C., Tapken, D., Werner, M., and Hollmann, M. (2009) *Neuroscience* **158**, 78–88
- Menuz, K., Stroud, R., Nicoll, R., and Hays, F. (2007) *Science* **318**, 815–817
- Soto, D., Coombs, I. D., Kelly, L., Farrant, M., and Cull-Candy, S. G. (2007) *Nat. Neurosci.* **10**, 1260–1267
- Bedoukian, M. A., Whitesell, J. D., Clay, C. M., and Partin, K. M. (2008) *J. Biol. Chem.* **283**, 1597–1600
- Chomczynski, P., and Sacchi, N. (1987) *Anal. Biochem.* **162**, 156–159
- Chu, P. J., Robertson, H. M., and Best, P. M. (2001) *Gene* **280**, 37–48
- Villmann, C., Bull, L., and Hollmann, M. (1997) *J. Neurosci.* **17**, 7634–7643
- Lee, J., Lee, H. J., Shin, M. K., and Ryu, W. S. (2004) *BioTechniques* **36**, 398–400
- Villmann, C., Strutz, N., Morth, T., and Hollmann, M. (1999) *Eur. J. Neurosci.* **11**, 1765–1778
- Chen, L., Chetkovich, D. M., Petralia, R. S., Sweeney, N. T., Kawasaki, Y., Wenthold, R. J., Brecht, D. S., and Nicoll, R. A. (2000) *Nature* **408**, 936–943
- Schnell, E., Sizemore, M., Karimzadegan, S., Chen, L., Brecht, D. S., and Nicoll, R. A. (2002) *Proc. Natl. Acad. Sci. U.S.A.* **99**, 13902–13907
- Bats, C., Groc, L., and Choquet, D. (2007) *Neuron* **53**, 719–734
- Honoré, T., Davies, S. N., Drejer, J., Fletcher, E. J., Jacobsen, P., Lodge, D., and Nielsen, F. E. (1988) *Science* **241**, 701–703
- Armstrong, N., and Gouaux, E. (2000) *Neuron* **28**, 165–181
- Schmid, S. M., Körber, C., Herrmann, S., Werner, M., and Hollmann, M. (2007) *J. Neurosci.* **27**, 12230–12241
- Wenthold, R. J., Petralia, R. S., Blahos, J., II, and Niedzielski, A. S. (1996) *J. Neurosci.* **16**, 1982–1989
- Mansour, M., Nagarajan, N., Nehring, R. B., Clements, J. D., and Rosenmund, C. (2001) *Neuron* **32**, 841–853
- Brorson, J. R., Li, D., and Suzuki, T. (2004) *J. Neurosci.* **24**, 3461–3470
- Strutz-Seebohm, N., Seebohm, G., Korniychuk, G., Baltaev, R., Ureche, O., Striegel, M., and Lang, F. (2006) *Pflugers Arch.* **452**, 276–282
- Yelshansky, M. V., Sobolevsky, A. I., Jatzke, C., and Wollmuth, L. P. (2004) *J. Neurosci.* **24**, 4728–4736
- Robert, A., Irizarry, S. N., Hughes, T. E., and Howe, J. R. (2001) *J. Neurosci.* **21**, 5574–5586
- Sun, Y., Olson, R., Horning, M., Armstrong, N., Mayer, M., and Gouaux, E. (2002) *Nature* **417**, 245–253
- Cokić, B., and Stein, V. (2008) *Neuropharmacology* **54**, 1062–1070
- Jin, R., Banke, T. G., Mayer, M. L., Traynelis, S. F., and Gouaux, E. (2003) *Nat. Neurosci.* **6**, 803–810
- Robert, A., Armstrong, N., Gouaux, J. E., and Howe, J. R. (2005) *J. Neurosci.* **25**, 3752–3762
- Tomita, S., Shenoy, A., Fukata, Y., Nicoll, R. A., and Brecht, D. S. (2007) *Neuropharmacology* **52**, 87–91
- Kohda, K., Wang, Y., and Yuzaki, M. (2000) *Nat. Neurosci.* **3**, 315–322
- Taverna, F., Xiong, Z. G., Brandes, L., Roder, J. C., Salter, M. W., and MacDonald, J. F. (2000) *J. Biol. Chem.* **275**, 8475–8479